



Universiteit
Leiden
The Netherlands

Enhancing reovirus for use in oncolytic virotherapy

Kemp, V.

Citation

Kemp, V. (2019, February 7). *Enhancing reovirus for use in oncolytic virotherapy*. Retrieved from <https://hdl.handle.net/1887/68327>

Version: Not Applicable (or Unknown)

License: [Licence agreement concerning inclusion of doctoral thesis in the Institutional Repository of the University of Leiden](#)

Downloaded from: <https://hdl.handle.net/1887/68327>

Note: To cite this publication please use the final published version (if applicable).

Cover Page



Universiteit Leiden



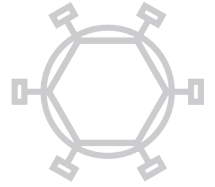
The following handle holds various files of this Leiden University dissertation:

<http://hdl.handle.net/1887/68327>

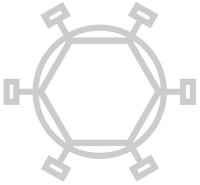
Author: Kemp, V.

Title: Enhancing reovirus for use in oncolytic virotherapy

Issue Date: 2019-02-07



6



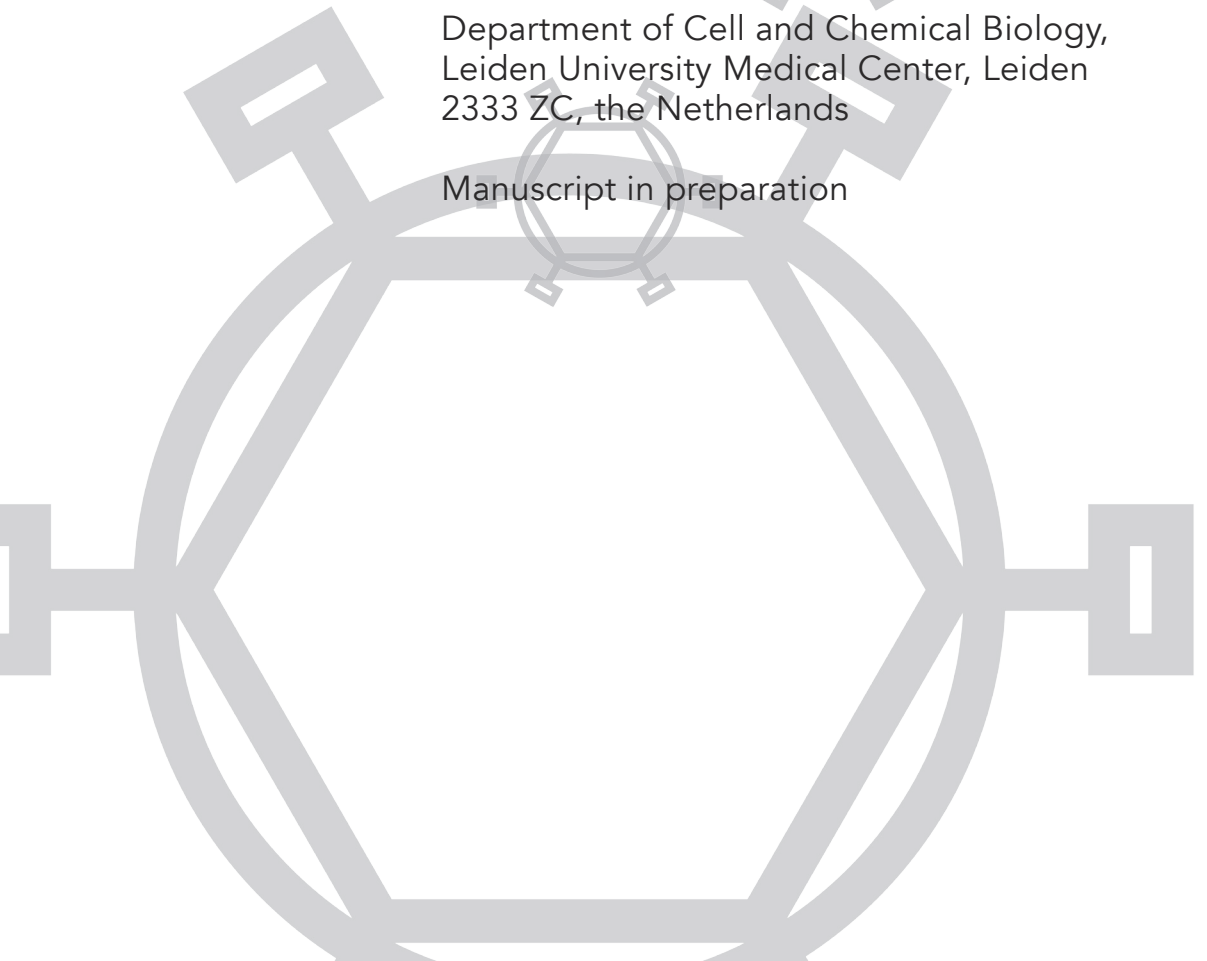
Yields and genetic stability of replicating recombinant reoviruses



Vera Kemp, Diana J.M. van den Wollenberg,
Ronald W.A.L. Limpens, Steve J. Cramer, Rob
C. Hoeben

Department of Cell and Chemical Biology,
Leiden University Medical Center, Leiden
2333 ZC, the Netherlands

Manuscript in preparation



ABSTRACT

Wild-type (wt) mammalian orthoreovirus Type 3 Dearing (T3D) has shown evidence of clinical activity as an oncolytic agent in cancer therapy, but its therapeutic efficacy remains to be augmented. Using a reverse genetics method, replication-competent reoviruses can be generated that encode a potentially therapeutic transgene. Insight into the infectivity and genetic stability of these modified reoviruses are prerequisites for their clinical use. We generated a series of transgene-containing reoviruses by replacing part of the spike protein σ 1-encoding segment by heterologous sequences. Although these recombinants could be propagated and stocks of recombinant reoviruses could be produced with relative ease, two phenomena currently limit their implementation in clinical translation programs. We observed a 10- to 750-fold lower infectious yield compared to wt T3D virus stocks. This was attributed to a lower infectivity of the transgene-containing reoviruses as the particle yields were similar to the wt viruses. We propose that the truncation of σ 1 hampers its stable insertion into the capsid and thereby negatively affects infectivity of the recombinant reoviruses. Moreover, occasionally mutants with deletions in S1 appeared from which transgene- and sometimes virus-derived sequences had been lost. The size of the deletions ranged from 47 to 519 nucleotides in length. The deletion mutants reveal the minimally required sequences for efficient packaging of modified segments into reovirus capsids. Our data suggest that the S1 RNA structure is underlying the deletions. Although medium-sized batches can be produced for preclinical research, routine monitoring of genome and particle integrity is essential when producing replication-competent reoviruses containing heterologous transgenes.

INTRODUCTION

Mammalian orthoreovirus T3D, hereafter called reovirus, is a non-enveloped virus harboring a segmented double-stranded RNA genome with a total length of 23.5 kb [1]. The name reovirus is an acronym of *respiratory and enteric orphan virus*, to indicate the sites of infection and the notion that the virus has not been associated with severe pathology in humans. In cell culture, reovirus infection usually initiates a lytic replication cycle and preferentially infects and lyses transformed cells. The tumor cell preference can be attributed to the inhibition of innate immune sensing by an activated RAS signaling pathway, and the stimulation of virus uncoating, genome replication, virus egress and the induction of apoptosis. These factors have contributed to the adoption of this virus as a candidate anti-cancer agent for various cancer types.

While the results of the clinical trials published so far demonstrate the safety and feasibility of this approach, the anti-cancer efficacy as a stand-alone therapy remains to be improved [2]. On the one hand this may be accomplished by increasing the infection efficiency of the viruses, especially in tumors with a downregulated expression level of the canonical reovirus receptor junction adhesion molecule-A (JAM-A). Alternatively, the anti-cancer potency may be improved by inserting a therapeutic transgene in the reovirus genome.

Recently, a strategy has been developed that allows the insertion of transgenes in the reovirus genome without increasing the size of the recipient reovirus genome segment. This was achieved by exploiting a unique feature of the *jin* mutant reoviruses, which have the capacity to infect cells independent of the presence of the JAM-A receptor on the cell surface [3]. The causative mutations locate in the S1 segment which encodes the viral spike protein $\sigma 1$. The mutations affect the shaft region of $\sigma 1$, clustering in the region that interacts with sialic acids on the host cell surface. We showed that the mutations increase the affinity of $\sigma 1$ for sialic acids, allowing the virions to undergo endosomal uptake independent of a high-affinity ligation to the JAM-A receptor. The head domain of $\sigma 1$ mediates interactions with JAM-A but it is not essential for spike protein trimerization [4]. Since the *jin* mutants do not rely on ligation of $\sigma 1$ to JAM-A for infection, the S1 region encoding the $\sigma 1$ head domain can be replaced by heterologous sequences. This allows the insertion of up to 450 bp of heterologous sequences without exceeding the size of the unmodified S1 segment. In this approach the codons for the non-structural protein $\sigma 1s$, which overlaps the $\sigma 1$ open reading frame but is read from another frame, is left intact. The feasibility and efficiency of this approach have been elegantly demonstrated by generating a reovirus in which the codons for the $\sigma 1$ head domain were replaced by a sequence encoding the 13 kDa fluorescent protein iLOV [5]. To achieve simultaneous expression of the $\sigma 1$ spike and of iLOV, a

poly-cistronic expression system exploiting the ribosomal skipping 2A sequence derived from the porcine tescho-1 virus (P2A) was used. This resulted in the separate synthesis of the truncated spike and the iLOV reporter protein.

We have expanded this approach to generate a number of replication-competent expanded-tropism reoviruses that harbor a heterologous transgene, without the need of a helper cell line expressing the modified genome segment [5-7]. A prerequisite for further clinical development of these recombinant viruses is that they can be produced to high titers and stably carry the transgene. In our routine propagation of transgene-containing reovirus batches, we observed a lower infectivity compared to wild-type reovirus and *jln* mutants. Moreover, a number of deletion mutants occurred, in which (parts of) the transgene and occasionally reovirus-derived sequences were deleted. Here, we describe the reduced infectivity of the reoviruses in which a transgene replaces the codons for the head domain of $\sigma 1$. Moreover we characterized a series of spontaneous deletion mutants that were found in batches of recombinant reoviruses and we speculate on the mechanisms involved in their generation.

MATERIALS AND METHODS

Cell lines and viruses

The cell lines U118-MG (obtained from ATCC, Manassas, VA, USA) and 911 [8] were cultured in high glucose Dulbecco's Modified Eagle's Medium (DMEM; Invitrogen, Life Technologies, Bleiswijk, the Netherlands), supplemented with 8% fetal bovine serum (FBS; Invitrogen) and with penicillin and streptomycin (pen-strep) as described [8, 9]. The 911scFvHis cells were generated by transduction of 911 cells with the lentivirus vector pLV-scFvHis-IRES-Neo as described before [10]. The resulting polyclonal cell line was cultured in DMEM containing 8% FBS, pen-strep and 400 $\mu\text{g}/\text{mL}$ G418. The T7-RNA polymerase-expressing cell line BSR-T7 [11] was provided by K. Conzelmann and cultured in DMEM, 8% FBS, pen-strep and 400 $\mu\text{g}/\text{mL}$ G418. All cell cultures were maintained in an atmosphere of 5% CO_2 at 37°C.

The wild-type Type 3 Dearing (wt T3D) reovirus strain R124 was isolated from reovirus T3D stock VR-824 from the ATCC (stock VR-824) by two rounds of plaque purification and propagated on 911 cells. Hereafter, this virus is referred to as wt T3D. The viruses were quantitated by plaque assays on 911 cells as described and virus concentrations and MOIs were defined on the basis of these titers [12]. For our experiments, we used cleared freeze-thaw lysates as reovirus stocks, unless indicated otherwise. Cesium chloride (CsCl) purified batches were generated as described before [7].

Generation of transgene-containing S1 segments

The recombinant reoviruses were constructed essentially as was described before [5-7]. Synthetic S1 segments were designed *in silico* and a DNA copy was synthesized by Eurofins MWG Operon (Ebersberg, Germany). The segment sequences were designed to contain the following features: (1) nucleotides (nts) 1 to 768 from the S1 segment of reovirus mutant *jin-3*; this includes the 5'-untranslated region, entire $\sigma 1$ s open reading frame (ORF) and the first 252 amino acids of the *jin-3* $\sigma 1$, including the codons for the G196R change near the sialic acid binding domain; (2) the codons for a 6 \times His-tag (18 bp), which is placed in-frame with the $\sigma 1$ -encoding part; (3) the codons for the porcine teschovirus-1 2A (P2A) sequence (66 bp +3 additional bp); followed by the (4) transgene with its stop codon; and (5) downstream of the transgene the 3' end of the S1 segment from nt 1219 to 1416 of wt T3D, which include A-, B- and C-box elements predicted to facilitate encapsidation of the reoviral positive strand ssRNA in the capsid [13, 14], as well as the 3'-untranslated region. The recombinant viruses rS1-mmGMCSF and rS1-hsGMCSF(co) contain the C-box but not the A- and B-boxes.

The fusion constructs were PCR cloned into the pBACT7 backbone of pBacT7-S1T3D as described before [5-7]. Plasmid pBacT7-S1T3D was purchased at Addgene (Cambridge, MA, USA) (plasmid 33282, <http://www.addgene.org>). The resulting plasmid was characterized by restriction analysis and a single clone was expanded and used for virus generation.

Generation of recombinant reoviruses

For the generation of recombinant reoviruses, we used the procedure described by Boehme *et al.* [15] with some modifications [5]. Whereas the original system uses 10 plasmids for providing the full complement of reovirus segments [16], our approach uses five plasmids. In addition to pBT7-modified S1, we used the following plasmids, pT7-L1T1L (Addgene, plasmid #33286), pT7-L2-M3T3D (Addgene, plasmid #33300), pT7-L3-M1T3D (Addgene, plasmid #33301) and pT7-M2-S2-S3-S4T3D (Addgene, plasmid #33302). For generating recombinant reoviruses, the five plasmids were transfected into BSR-T7 cells using the TransIT-LT1 transfection reagent (Mirus; Sopachem BV, Ochten, the Netherlands), according to the manufacturer's manual.

At 72 hours post transfection, the cells were harvested and lysed by three cycles of freeze-thawing. After pelleting the cell debris, the cleared supernatant containing the recombinant reoviruses was added to 911scFvHis cells in a 6-well plate. Upon the first appearance of cytopathic effect (CPE), the cells were harvested and the recombinant reovirus was released from the cells by three cycles of freeze-thawing. The cell debris was removed from the reovirus-containing lysate by

centrifugation (10 min at 3000g), and stored at -20°C until further use. The virus was routinely passaged by exposing fresh semi-confluent cultures of 911scFvHis cells to dilutions of the cleared lysates.

Medium-sized batches of cesium chloride (CsCl) purified recombinant reoviruses were prepared as described before [7]. The CsCl-purified reoviruses were recovered in reovirus storage buffer (RSB: 10 mM Tris-HCl pH 7.5, 150 mM NaCl, 10 mM $\text{MgCl}_2 \cdot 6\text{H}_2\text{O}$) supplemented with 0.1% Bovine Serum Albumin (BSA), and were aliquoted and stored at 4°C until use. The amount of particles was calculated based on the OD_{260} values. The infectious titers were determined based on TCID_{50} assays as described before [5].

For routine production, the reoviruses were amplified by infecting near-confluent cultures of 911 cells or 911scFvHis cells at an MOI of 2-5 and harvesting the cells after 48 - 64 hours depending on the progression of the cytopathic effects in the cultures. Upon harvesting the combined cells and medium, the harvest was freeze-thawed 3 times and the lysate was cleared by low-speed centrifugation.

Reverse transcriptase PCR and sequence analysis

911scFvHis cells were infected with the recombinant reoviruses. As we had no indication of the titer of the early passaged batches (P1 of the recombinant viruses) obtained upon the initial transfection experiment, 1/20th part of the isolated viruses was used for exposure of the cells. Total RNA was extracted from the infected cells with the Absolutely RNA Miniprep Kit (Stratagene, Agilent Technologies, Amstelveen, the Netherlands) according to the manual. Subsequently, cDNA was synthesized using the S1EndR primer (5'-GATGAAATGCCCCAGTGC-3') and SuperScript III reverse transcriptase (Invitrogen, Life Technologies). In the PCR, the following primers were used to detect S1: S1For – 5'-GCTATTGGTCGGATGGATCCTCG-3' – and S1EndR, with GoTaq polymerase (Promega, Leiden, the Netherlands). The positions of the primer binding sites are shown in Supplementary figure 1.



Supplementary figure 1. Primer locations on S1 for S1 RT-PCR analysis. Schematic representation of the PCR analysis, showing the S1 segment, the locations of the primers S1For and S1EndR, and the length of the PCR fragment.

For sequence analysis, Pfu DNA polymerase (Fermentas, FisherScientific, Landsmeer, the Netherlands) was used to amplify the genome segments and the PCR products of the S1 segments were sent to the Leiden Genome Technology Center (Leiden University Medical Center, Leiden, the Netherlands) for Sanger sequencing. Primers used in the sequence reactions were S1For and S1EndR.

Electron microscopy

For electron microscopy analyses, reovirus batches were fixed in 0.75% Glutaraldehyde in 0.1 M cacodylate buffer for 30 minutes at room temperature. Subsequently, they were adsorbed for 1 minute to freshly glow-discharged, carbon-coated pioloform grids, followed by negative staining with a 2% phosphotungstic acid (PTA) solution for 30 seconds. Analyses were performed using a Tecnai 12 electron microscope (FEI) at 120 kV, equipped with a 4K OneView CMOS Camera (Gatan).

Western blot

Purified virus particles were subjected to western blot analysis. Western sample buffer (final concentration: 10% glycerol, 2% SDS, 50 mM Tris-HCl pH 6.8, 2.5% β -mercaptoethanol and 0.025% bromophenol blue) was added to 1×10^9 or 1×10^{10} viral particles (based on OD₂₆₀ measurements) in RSB. Samples were heated for 3 minutes at 97°C before loading on a 10% polyacrylamide-SDS gel. The proteins were transferred to Immobilon-PSQ (Merck-Millipore, Amsterdam, the Netherlands) for detection with the Odyssey system (LI-COR Biotechnology, Westburg, Leusden, the Netherlands). Separate blots were prepared for the detection of $\sigma 1$ (blot 1), and $\lambda 2$ (blot 2). Primary antibody used to detect $\lambda 2$ (7F4) was obtained from the Developmental Studies Hybridoma Bank developed under the auspices of the NICHD and maintained by the University of Iowa, Department of Biology [17]. Primary antibody against the $\sigma 1$ tail was described before [5]. Blot 2 was re-stained for P2A, using a rabbit anti-P2A peptide serum ABS31 (Merck-Millipore, Amsterdam, the Netherlands). For the detection of the primary antibodies, the IRDye 800CW Donkey-anti-Rabbit IgG and IRDye 680RD Donkey-anti-Mouse IgG (LI-COR Biotechnology, Westburg BV, Leusden, the Netherlands) were used.

ISVP experiment

Intermediate subviral particles (ISVPs) of rS1-mmGMCSF and wt T3D were generated as described previously [3]. In short, both viruses were diluted to $\sim 5 \times 10^{11}$ particles/ml, and incubated with 200 $\mu\text{g}/\text{mL}$ α -chymotrypsin (C3142, Sigma) at 37°C for 1 hour. Subsequently, the reaction was stopped by addition of 5 mM PMSF

(78830, Sigma) at 4°C. The control rS1-mmGMCSF and wt T3D were diluted to the same extent as the ISVPs by adding the same volumes of RSB.

911 cells were seeded in 24-well plates at 3×10^5 cells/well. Each well was mock-treated or infected with ISVP-mmGMCSF, rS1-mmGMCSF, ISVP-T3D, or wt T3D at 2×10^4 particles/cell. After 1 hour incubation at 4°C to synchronize the infection, cells were incubated for 5 hours and 24 hours at 37°C. Then, the cells were permeabilized in Perm/Wash buffer (BD Biosciences) for 15 minutes at room temperature, spun down, and stained for reovirus $\sigma 3$ protein. Used antibodies are Mouse-anti- $\sigma 3$ (4F2), and PE-conjugated Goat-anti-Mouse (BD Biosciences). Each condition was measured in duplicate.

RESULTS AND DISCUSSION

Construction of recombinant reoviruses

Genetic modification of reovirus has been greatly facilitated by the development of the plasmid-based reverse genetics strategy. We previously described the generation of reoviruses expressing the fluorescent reporter iLOV (rS1-iLOV) [5], the oncolytic E4orf4 (rS1-E4orf4), its inactive variant RFA (rS1-RFA) [6], human GM-CSF (rS1-hsGMCSF) and murine GM-CSF (rS1-mmGMCSF) [7]. As illustrated in Figure 1a, BSR-T7 cells were transfected with plasmids encoding the different reovirus segments. The cells were harvested after 72 hours and the lysates were added to 911scFvH cells for virus amplification. As illustrated in Figure 1b, we replaced the codons for the $\sigma 1$ head domain, which is responsible for binding to the canonical reovirus receptor junction adhesion molecule-A (JAM-A), for generating reoviruses carrying the transgene of interest. Furthermore, the constructed S1 segments contain a G196R mutation that we previously identified in the *jin-3* reovirus mutant [3]. This mutation mediates JAM-A independent entry through enhanced sialic acid binding. To allow for the separate synthesis of the $\sigma 1$ and the heterologous protein, a porcine teschovirus-1 2A (P2A) sequence was incorporated. Lastly, the codons for a 6x His tag were inserted to augment initial propagation in 911scFvH cells harboring a His receptor [10].

During the construction of the recombinant S1 segments, we took care not to exceed the 1416 base pairs (bp) length of the wild-type (wt) Type 3 Dearing (T3D) S1 segment. As can be seen in Figure 1b, all successfully generated recombinant viruses contain a S1 segment within this size, except for the viruses harboring S1His-2A-E4orf4 and S1His-2A-RFA which are only 3 bp longer (*i.e.* 1419 bp). Our attempts to generate batches of recombinant reoviruses harboring the codons for either DsRed [5] or Gaussia Luciferase with S1 segment sizes of 1722 bp and 1539 bp, respectively, were unsuccessful despite various attempts. We concluded that a

considerable increase in the length of the S1 segment hampers the production of these reoviruses.

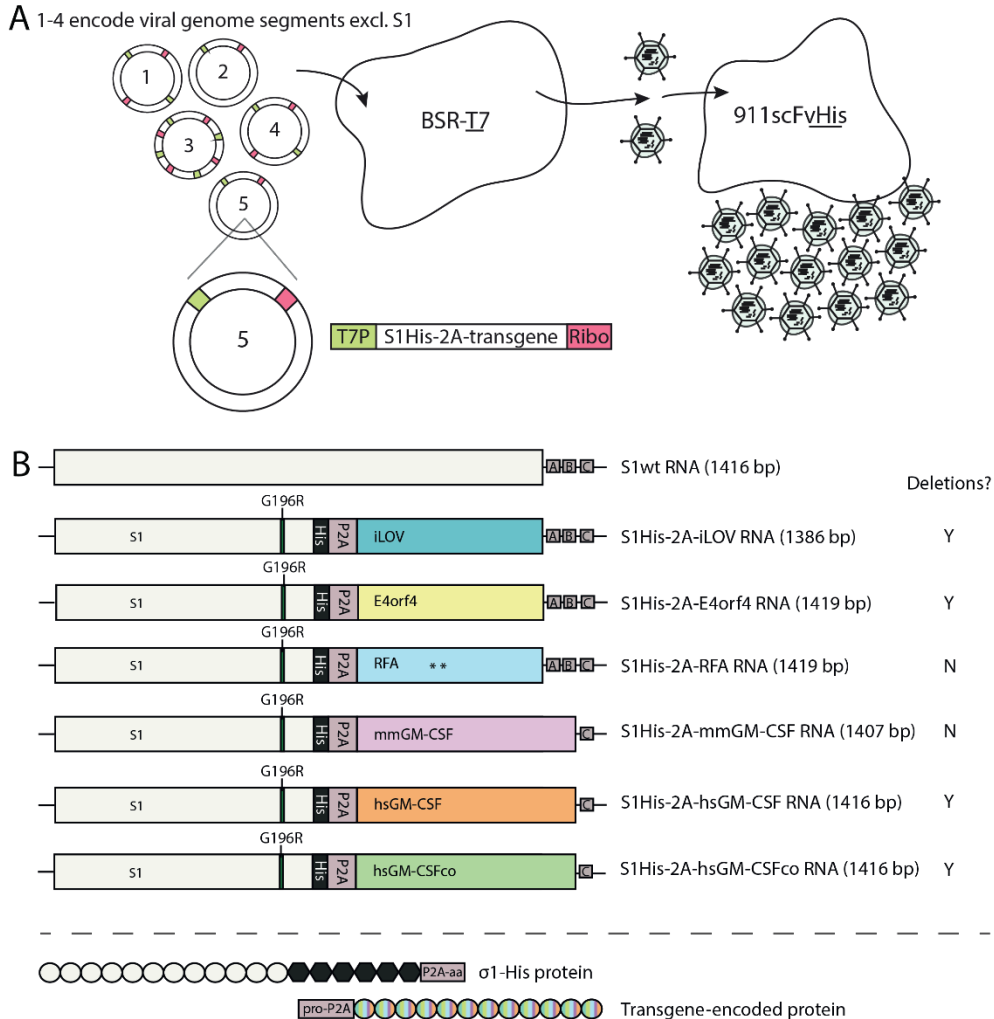


Figure 1. Overview of the generation of recombinant reoviruses and the constructed S1 segments. A) For the generation of recombinant reoviruses, BSR-T7 cells were transfected with 4 plasmids encoding the different reovirus segments except for S1, and the pBT7-modified S1 segment encoding the transgene of interest. The cells were harvested after 72 hours and the lysates were added to 911scFvH cells for virus amplification. B) The modified S1 segments encoding the different transgenes, adapted from Kemp *et al.* 2018 [7]. The

segment sequences were designed to contain the following features: (1) nucleotides (nts) 1 to 768 from the S1 segment of *jln-3*; harboring the 5'-UTR, entire $\sigma 1$ s ORF and the first 252 amino acids of the *jln-3* $\sigma 1$, including the codons for the G196R change near the sialic acid binding domain; (2) the codons for a 6 \times His-tag (18 bp); (3) the codons for the P2A sequence; followed by the (4) transgene encoding the heterologous protein – iLOV, E4orf4, RFA, mmGM-CSF, hsGM-CSF, and hsGM-CSFco – including a stop codon. Downstream of the transgene (5) the 3' end of the wt T3D S1 segment, which includes the A-, B- and C-box elements predicted to facilitate encapsidation of the reovirus positive strand ssRNA in the capsid [13, 14], as well as the 3'-UTR. The recombinant viruses rS1-mmGMCSF and rS1-hsGMCSF(co) contain the C-box but not the A- and B-boxes. The occurrence or absence of deletion mutants is indicated by Y (yes) or N (no), respectively.

Production and stability of virus particles

During the routine production, we noted that the infectious titers of our purified recombinant reovirus batches were relatively low compared to batches of wt T3D reovirus or mutants such as *jln-3* (representative examples of the obtained yields per T75 flask in Table 1). Initially, we were unable to purify the recombinant viruses due to the absence of a clear virus band in the CsCl gradient. However, the freeze-thawed virus-containing cell lysates did contain infectious viruses prior to purification, as demonstrated by titrations based on TCID₅₀ assays (examples in Table 1). We had implemented benzonase treatments in our purification protocol, to remove undesired free nucleic acids. For optimal benzonase activity during our purifications, the buffer in which the viruses are harvested had a NaCl concentration of 100 mM. While this procedure yields very pure and concentrated stocks for the wt reovirus, we lost the *jln* mutant viruses and the transgene-containing viruses. We speculated that the G196R mutation responsible for enhanced sialic acid binding mediates negative charge dependent binding to cellular debris (membranes, DNA, RNA, etc.). As the cellular debris will be cleared from the cell lysate during Vertrel extractions, the *jln* and transgene-containing reoviruses would be lost prior to CsCl purification. We could remedy this by increasing the salt concentration of the harvest buffer to 250 mM NaCl. This retained benzonase activity and presumably sufficiently weakens the charge-dependent bonds between the viruses and the cellular debris. Indeed, after this amendment of the protocol we obtained clear virus bands upon CsCl purification with all reoviruses.

Importantly, despite the now similar particle yields of the transgene containing reoviruses, the infectious titers were approximately a 10-750 fold lower than those of wt T3D and *jln* reoviruses. Typically, we obtained roughly 10⁸ infectious units (IU) of recombinant reovirus from 1 infected T75 flask of 911 or 911scFvH cells, compared to around 10¹⁰ IU for wt T3D or *jln* reoviruses. However, the particle yields

as measured by the OD₂₆₀ values were similar, demonstrating that similar amounts of virus particles were produced. As a result, the particle-to-IU ratios of the recombinant virus batches were relatively high (usually around 10000:1 compared to 100:1 for *jin* mutants and wt T3D). Moreover, we found that the infectivity of the transgene-containing reoviruses decreased in time (approximately 1000-fold in 6 months) upon storage at 4°C. This could be fully remedied by the inclusion of 0.1% BSA in the reovirus storage buffer. This suggested that the inactivation may have been caused by aggregation of the recombinant reovirus particles.

Virus	Purified	Yield (IU/flask)
T3D	Yes	1.14x10 ¹⁰
<i>jin-3</i>	Yes	1.27x10 ¹⁰
rS1-iLOV	Yes	1.83x10 ⁸
rS1-iLOV	No	1.03x10 ⁸
rS1-mmGMCSF	Yes	9.91x10 ⁷
rS1-mmGMCSF	No	1.74x10 ⁸

Table 1. Yields obtained for wt T3D and recombinant reoviruses. Table overview of examples of yields obtained for batches of wt T3D, *jin-3*, and recombinant reoviruses rS1-iLOV and rS1-mmGMCSF. Infectious yields are displayed as infectious units (IU) per T75 flask and are representative for the various produced virus batches.

Differences in morphology of rS1-mmGMCSF and wt T3D reoviruses

To examine potential differences in the overall appearance of recombinant reovirus and wild-type reovirus particles, we used electron microscopy of purified rS1-mmGMCSF and wt T3D reovirus particles. As can be seen in Figure 2, the virus particles of rS1-mmGMCSF and wt T3D appeared similar in morphology and size. No increase in the abundance of electron-dense empty particles was seen for rS1-mmGMCSF. A closer examination of the particles revealed a potential difference in appearance, with a fuzzy outer capsid displaying ‘dark spots’ on the rS1-mmGMCSF particles but not the wt T3D particles. Possibly, these electron-dense areas represent empty locations in the reovirus outer capsid in which the dye concentrated. This suggests that a capsid protein, most likely $\sigma 1$, is not stably incorporated. For the structurally similar adenovirus, it has been shown that truncation of its fiber protein leads to a decreased stability and faster disassembly of the viral particle [18]. If this

also is the case for the truncated $\sigma 1$ in our recombinant reoviruses, it could be that the viral capsid of rS1-mmGMCSF is intrinsically less stable than that of wt T3D.

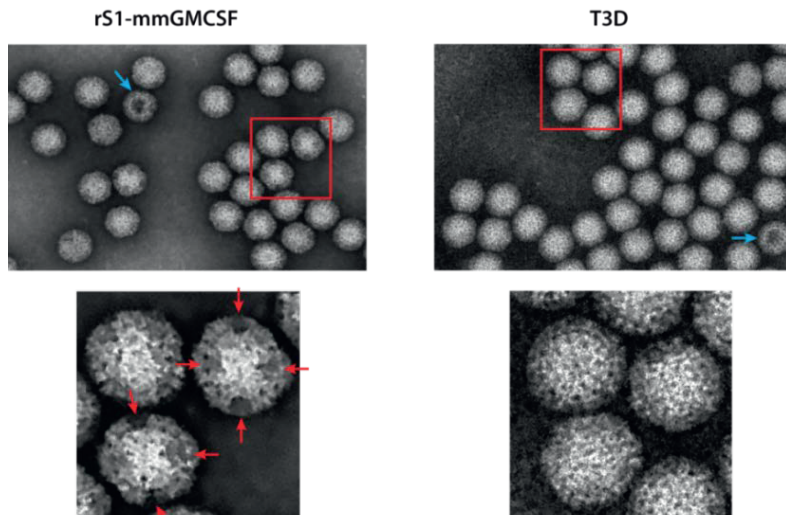


Figure 2. Electron microscopic pictures of rS1-mmGMCSF and wt T3D particles. Purified reovirus batches were fixed and adsorbed to carbon-coated grids, followed by negative staining. Electron microscopic photographs were taken. The lower pictures represent zoomed in parts of the upper photographs (red boxes). Electron-dense spots on the outer capsid are indicated by red arrows. Blue arrows indicate empty virus particles.

Expression levels of capsid proteins in purified rS1-mmGMCSF and wt T3D particles

We hypothesized that the truncated $\sigma 1$ is expressed in the viral particle, and thereby should be able to mediate viral entry. However, its truncated form may interfere with capsid integrity by affecting the stability of its own trimerized form or of interacting capsid protein $\lambda 2$. The reovirus $\lambda 2$ protein is implicated in $\beta 1$ -integrin mediated internalization [19]. Destabilization of this protein in the capsid may therefore hamper infectivity. We performed a semi-quantitative western blot analysis on the expression levels of $\sigma 1$ and $\lambda 2$ in purified reovirus particles, comparing rS1-mmGMCSF with wt T3D. Notably, we did not see differences in the expression levels of $\lambda 2$ (Figure 3), suggesting that the truncated $\sigma 1$ does not influence the stability and abundance of this neighboring capsid protein.

It has been shown that the N-terminal fibrous proportion of $\sigma 1$ is able to form trimers [4]. Although there are contradictory reports [20], truncations of $\sigma 1$ can sometimes result in reduced levels of $\sigma 1$ in the capsid [21]. We speculated that encapsidation of the truncated $\sigma 1$ protein in our recombinant reoviruses may be

reduced, resulting in a lower $\sigma 1$ abundance in the capsid. Possibly, not all vertices are occupied by $\sigma 1$ trimers. To see whether the amount of $\sigma 1$ in the capsid is reduced by the truncation, we compared the $\sigma 1$ levels in the purified rS1-mmGMCSF and wt T3D particles. Indeed, purified rS1-mmGMCSF particles seem to harbor a lower level of truncated $\sigma 1$ ($\sigma 1$ -trunc) compared to the level of full-length $\sigma 1$ ($\sigma 1$ -FL) in wt T3D particles (Figure 3). As $\sigma 1$ -trunc expression in rS1-mmGMCSF particles was almost undetectable, we checked the P2A expression level to confirm the presence of $\sigma 1$ -trunc. We usually obtain stronger stained bands with the anti-P2A antibody compared to anti- $\sigma 1$ [5]. The detected P2A is attached to the $\sigma 1$ -trunc protein, so can be used as a different measure of $\sigma 1$ -trunc expression. Indeed, P2A bands were clearly identified in the rS1-mmGMCSF particles, confirming that $\sigma 1$ -trunc is present, albeit possibly at a low level. Taken together, we propose that the truncation of $\sigma 1$ does not influence the stability of neighboring capsid proteins, but instead seems to inhibit its own stable insertion into the capsid. Interestingly, it has been demonstrated that three $\sigma 1$ trimers per virion are the minimum to retain full infectivity [22]. It remains to be determined whether the truncated $\sigma 1$ proteins in our recombinant reoviruses are able to trimerize, and if so, how many $\sigma 1$ trimers are stably present in the viral capsid. The semi-quantitative western blot analysis does not give a decisive answer to this. Instable spike trimers could lead to the leakage of RNA from the viral particles. As we did not observe an increase in the amount of empty particles in rS1-mmGMCSF batches compared to wt T3D batches, there seems to be no dramatic increase in RNA leakage from the rS1-mmGMCSF particles. Future research is warranted to elucidate this phenomenon.

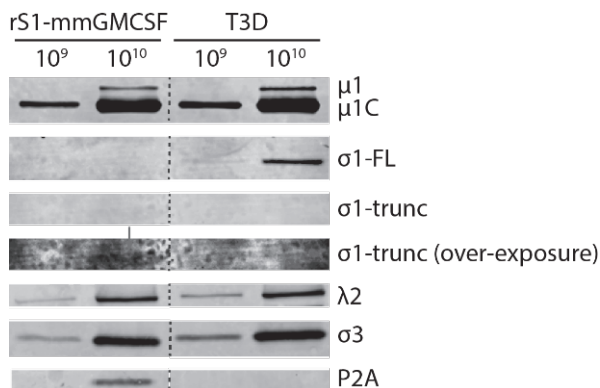


Figure 3. Expression of full-length $\sigma 1$, truncated $\sigma 1$, $\lambda 2$, and P2A in purified rS1-mmGMCSF and wt T3D particles. Purified virus (10^9 and 10^{10} particles) was subjected to a semi-quantitative western blot analysis of $\sigma 1$, $\lambda 2$, and P2A expression. Detection was performed using the Odyssey system. The red arrow indicates a faint $\sigma 1$ band.

6

Infectivity of rS1-mmGMCSF is not enhanced by ISVP generation

For adenovirus, it has been described that truncation of its fiber protein leads to a decreased adsorption onto, and entry into, cells [23]. We speculated that the truncation of the reovirus $\sigma 1$ protein reduces infectivity by hampering the cell entry capacity of the virions, either due to reduced levels of $\sigma 1$ in the capsid or through a direct effect of the truncation on the cell binding ability of $\sigma 1$. To test this hypothesis, we made intermediate subviral particles (ISVPs) of rS1-mmGMCSF (ISVP-mmGMCSF) and wt T3D (ISVP-T3D) reoviruses. ISVPs may enter cells independent from $\sigma 1$ binding to JAM-A and/or sialic acids [9]. Therefore, if truncation of the $\sigma 1$ spike interferes with entry, it is expected that ISVP-mmGMCSF would enter cells more efficiently than rS1-mmGMCSF. For wt T3D, this positive effect of ISVP generation on cell entry is expected to be lower, because wt T3D can already efficiently enter cells. To study the degree to which the reoviruses can enter cells, we checked the $\sigma 3$ expression in 911 cells at 5 and 24 hours upon infection with rS1-mmGMCSF, ISVP-mmGMCSF, wt T3D, or ISVP-T3D. As a control, U118-MG cells were taken along. U118-MG cells lack JAM-A expression and therefore resist wt T3D but not ISVP-T3D infection. Because of their S1 G196R mutation, both rS1-mmGMCSF and ISVP-mmGMCSF can infect U118-MG cells through enhanced sialic acid binding. Therefore, U118-MG cells can be used to check for successful ISVP generation. Indeed, ISVP generation of wt T3D increased the $\sigma 3$ expression in U118-MG cells. Surprisingly, we found no increase in $\sigma 3$ expression in infected 911 cells for both rS1-mmGMCSF and wt T3D upon ISVP generation (Figure 4). If anything, the original rS1-mmGMCSF and wt T3D reoviruses seem to enter more efficient than the ISVPs. These results indicate that the relatively low infectivity of rS1-mmGMCSF compared to wt T3D is not caused by a reduced cell penetration capacity, suggesting that a post-entry step is inhibited during infection with these recombinant reoviruses.

S1 deletion mutants

As indicated in Figure 1, several of the produced recombinant reoviruses acquired deletions during passaging. As described before, the deletion mutants overgrow the virus populations upon prolonged propagation, suggesting that they have a selective growth advantage over the intact recombinant reoviruses [7]. The overview in Figure 5 summarizes the sequences that were found deleted. The S1 sequences that were deleted provide insight into the elements that are dispensable for incorporation of the segment into the viral capsid. We previously reported the deletion of the A- and B-boxes in an rS1-iLOV deletion mutant, suggesting that these sequences are not essential for the formation of infectious reovirus [5]. This notion was strengthened by the successful generation of rS1-hsGMCSF and rS1-mmGMCSF in which the A- and

B-boxes were omitted from the recombinant segments [7]. Furthermore, rS1-hsGMCSF del3 reveals that a small proportion of the S1 segment upstream of the His-tag insertion, and including the trypsin cleavage site implicated in the trypsin-mediated conversion of reovirus virions to ISVPs, is non-essential [24]. As only 7 amino acids would be released protein upon trypsin digestion, this observation may not come unexpected.

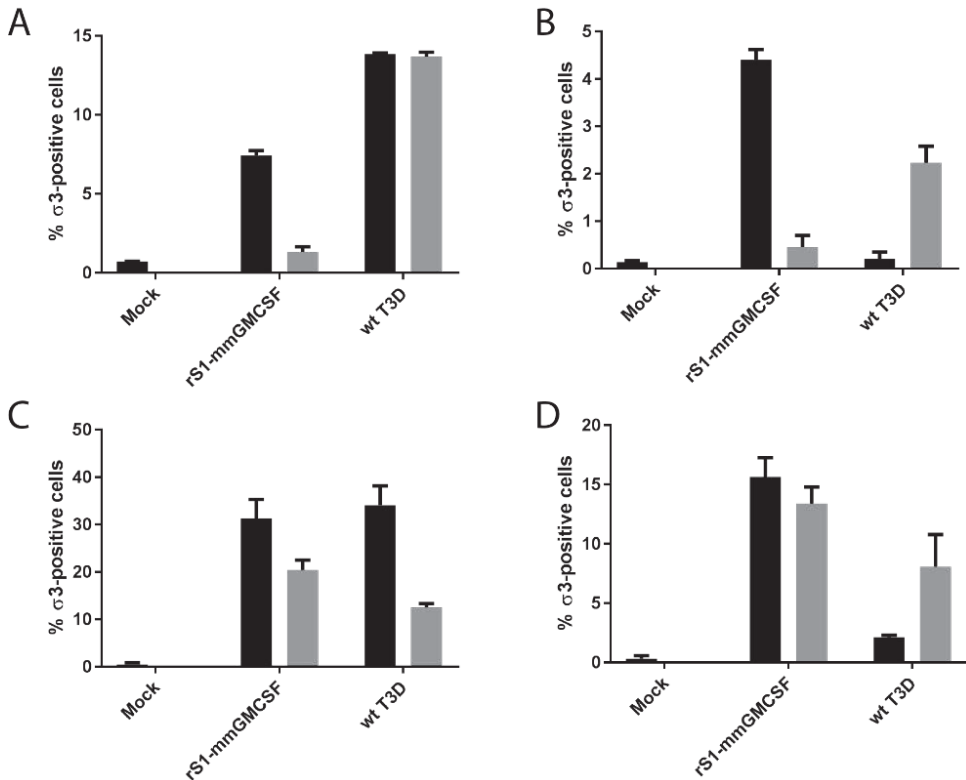


Figure 4. Percentage of $\sigma 3$ -positive 911 and U118-MG cells upon infection with ISVPs or normal rS1-mmGMCSF/wt T3D. ISVPs of rS1-mmGMCSF and wt T3D were generated by exposing $\sim 5 \times 10^{11}$ particles/ml to 200 $\mu\text{g}/\text{mL}$ α -chymotrypsin. The reaction was stopped by addition of 5 mM PMSF. Cultures of 911 (A, C) and U118-MG (B, D) cells were mock-treated or infected with ISVP-mmGMCSF, rS1-mmGMCSF, ISVP-T3D, or wt T3D at 2×10^4 particles/cell. After synchronization of the infection, cells were left for 5 hours (A-B) and 24 (C-D) hours. Then, the cells were stained for intracellular $\sigma 3$ protein. Each condition was measured in duplicate. Light grey bars represent ISVP treatments; black bars represent non-ISVP treatments.

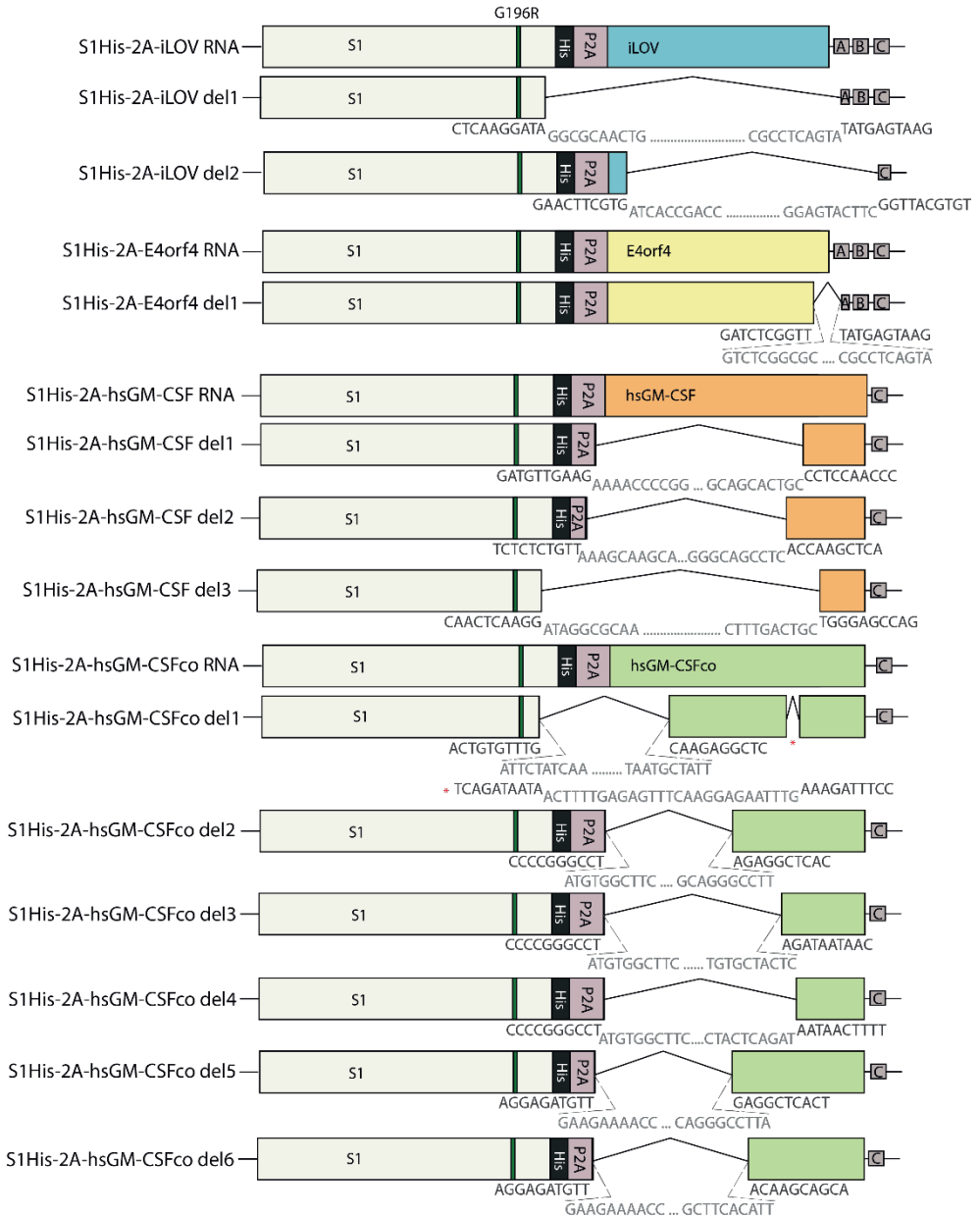


Figure 5. Overview of deletion mutants including sequences at the deletion junctions. Schematic overview showing the different deletions occurring in the recombinant reovirus batches. Indicated are the sequences at the junctions (retained sequence in black, deleted

sequence in grey). Various lengths of transgene-derived and occasionally reovirus-derived sequences were deleted.

S1 deletions are unlikely caused by replacing the S1 head domain or removing the A- and B-boxes

To gain more insight into the requirements for generating batches of genetically stable recombinant reoviruses, we need more insight into the mechanism(s) underlying the deletions. The fact that we find deletions for various recombinant reoviruses and their appearance in separate propagation experiments implies that the different deletions are caused by a pervasive mechanism. It seems unlikely that the deletions are merely an intrinsic consequence of replacing the S1 head domain by a transgene, as we only observed deletions in 3 of the 5 recombinant reoviruses. It can also be ruled out that it is an inevitable result of removal of the A- and B-boxes for the construction of the rS1-mmGMCSF and rS1-hsGMCSF(co) viruses, as deletions also occur in batches of rS1-iLOV and rS1-E4orf4, in which the A- and B-boxes have been retained.

S1 deletions are unlikely caused by adverse effects of the transgene-encoded protein

The deletion mutants overgrow the virus population within a few passages, suggesting that the removal of the transgene positively affects the viral replication cycle. We hypothesized that the deletion mutants could be the result of a negative effect of the transgene-encoded protein on the virus replication cycle. However, this seems unlikely because the deletions are found for a variety of transgenes. There is no evidence that would suggest that the iLOV fluorescent protein negatively influences viral replication and that therefore a deletion mutant has a growth advantage. For GM-CSF, it could be speculated that it influences cells expressing the GM-CSF receptor, and thereby affects viral replication in the cell culture. Although hsGM-CSF and mmGM-CSF proteins share 54% identity of their amino acid sequences, their biological activities are species-specific [25]. As we grow our reoviruses on a human cell line, and deletions were only observed for rS1-hsGMCSF and not rS1-mmGMCSF, a deleterious effect of hsGM-CSF could be underlying the sequence deletions. The GM-CSF receptor is generally expressed on a subset of immune cells specifically, but its expression on our propagation cell line 911 has never been tested and can therefore not be ruled out. To circumvent any effect of hsGM-CSF production on our production cell line, we attempted to generate the rS1-hsGMCSF virus on a non-human cell line. However, several attempts to stably propagate this virus on L929 cells failed, suggesting that the deletions are unrelated

to adverse effects of the transgene-encoded protein on the producer cell line (data not shown).

The mechanism responsible for generating the S1 deletions

There are two distinct mechanisms that could give rise to deletion mutants. In a first mechanism, sequences are removed from an existing RNA molecule. Such a mechanism would require the break of an internal phosphodiester bond, by a nuclease or in a non-enzymatic reaction, and subsequently the re-establishment of a new bond at another position. This reaction would require an RNA ligase, or a splicing type of reaction. Alternatively, the deletion may be resulting from a template switch or jump by the reoviral RNA-dependent RNA polymerase. The polymerase could stall and reinitiate the RNA synthesis at another part of the template. This would skip a part of the template and result in the loss of genetic information.

S1 deletions are unlikely caused by splicing-related events

A potential mechanism underlying the deletions could be splicing-mediated events. This process is typically thought to exclusively take place in the cell nucleus, but a growing number of transcripts has been found to undergo cytoplasmic splicing [26]. To see whether this could explain the S1 deletions in our recombinant reoviruses, we inspected the sequences flanking the deletions for the presence of splice sites (Figure 5). We have not found common sequences at the junctions and no similarity with any nuclear consensus splice site donor and acceptor sequences (5' GU and 3' AG) at the deletion junctions. In some cases, an AG sequence was apparent in the minus strand of the deletion (S1His-2A-iLOV del2 and S1His-2A-hsGM-CSFco del 3). The recognition of this site by the cytoplasmic splicing machinery seems doubtful, as the minus strand RNA of the reovirus genome is synthesized within the new viral cores and therefore should not reside free in the cytoplasm of the cell [1]. In conclusion, we have no evidence that cytoplasmic splicing causes the deletions.

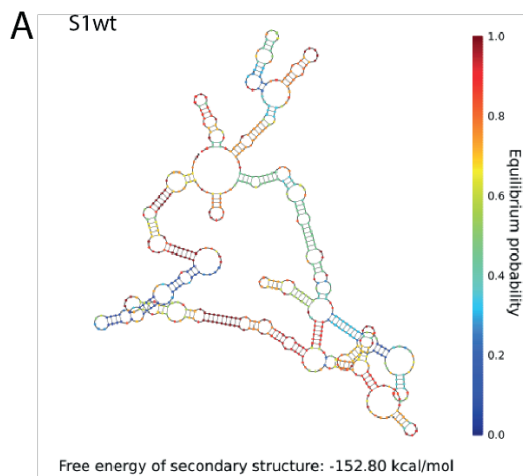
S1 deletions are unlikely caused by homology-related events

In one of the deletion mutants, rS1-hsGMCSF del2, we found some degree of homology between the six nucleotides flanking the 5' of the deletion (5' – GGGCCT – 3') and the final 3' seven nucleotides (5' – GGGCCTT – 3') of the deletion (Figure 5). Therefore, we hypothesized that homology-related events are causing the S1 segment deletion. However, for none of the other deletion mutants we have observed a substantial degree of homology in the sequences flanking the deletion or elsewhere in the S1 segment.

S1 deletions may be caused by complexities in RNA structure

We proposed that the underlying cause for the deletions may reside in complexities in the secondary or tertiary RNA structure of the transgene sequences in the S1 segment. As a result, deleting the sequences would increase the simplicity and stability of the S1 segment structure. Experimental validation and *in silico* prediction of the RNA structure is complex for relatively long sequence stretches (> 1000 nt) and the results are often unreliable. Also, we should realize that the transcription of the reovirus RNAs takes place on dsRNA templates.

Instead, one could analyze the smaller-sized deletions only. We compared the secondary RNA structures (<http://www.nupack.org>) and specifically their free energy values of the plus strand wild-type S1 sequence encoding the σ 1 head domain (Figure 6a) and the different transgenes (Figure 6b). As expected, it can be seen that codon-optimizing the hsGM-CSF sequence resulted in a lower negative free energy value, indicating that the codon-optimized version may have an advantage over the original sequence in terms of stability. Interestingly, the RNA structures of the successfully expressed transgenes had higher negative free energy values than the ones that have yielded deletions. The wild-type S1 sequence had a free energy value of -151.80 kcal/mol, the highest negative value of all structures analyzed. This suggests that the deletion mutants do not appear and overgrow the virus population due to harboring a more stable S1 RNA structure with a reduced negative free energy value. However, it should be noted that the structure analyses of only the transgenes could give a biased interpretation because it does not take into account the context of the rest of the S1 segment it is embedded in. Based on the variety and apparent randomness of the deletions, we propose that complexities in RNA structure still represent the most likely underlying cause of the deletions.



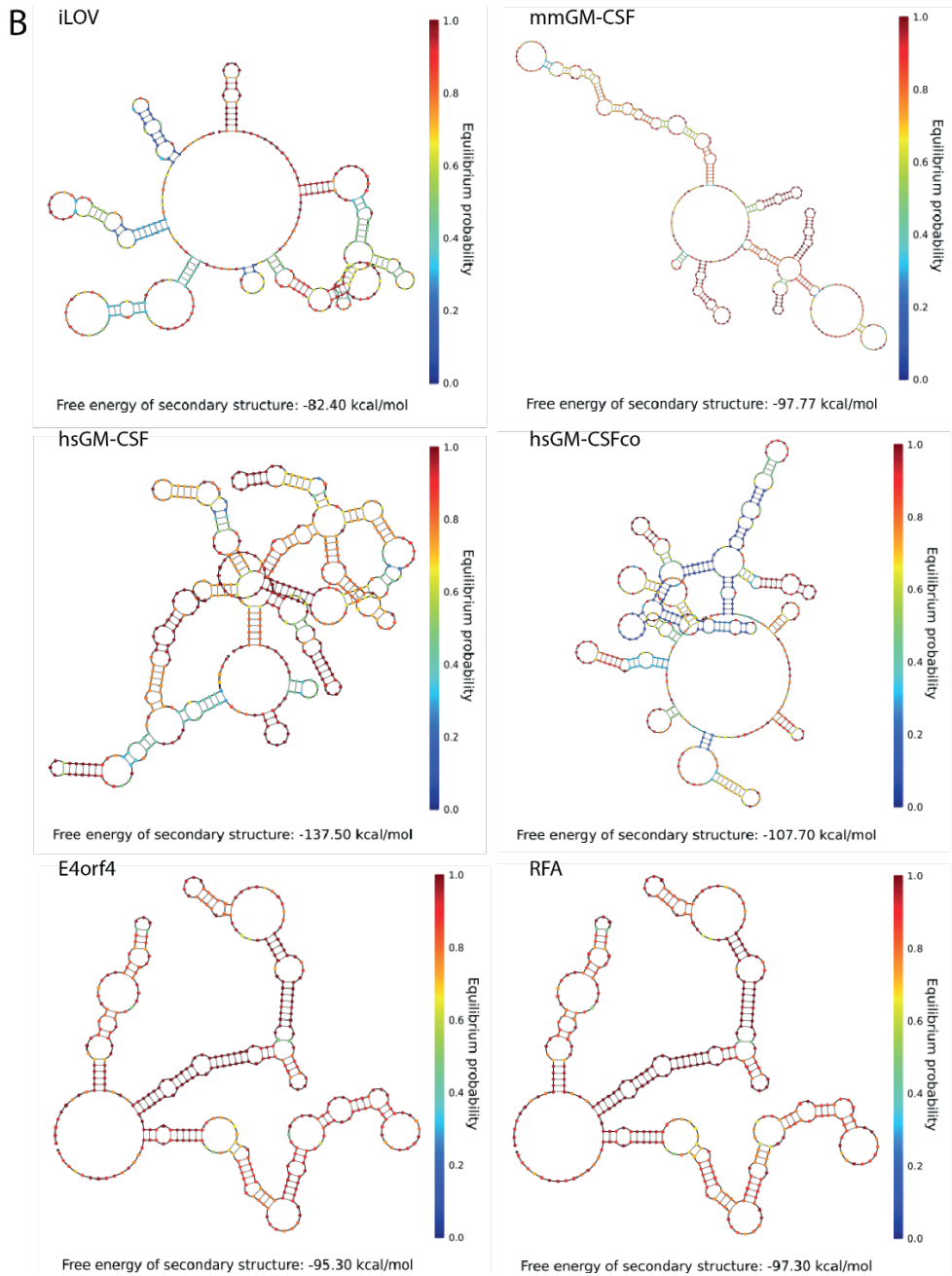


Figure 6. RNA structures of the wt S1 head domain region, and the different transgenes. Analysis of the RNA structure and free energy values of A) the wt S1 head domain region, and B) the different transgenes encoding iLOV, mmGM-CSF, hsGM-CSF, hsGM-CSFco, E4orf4, and RFA. Analysis was performed on <http://www.nupack.org>.

Alternatively, the modified genomes may exhibit stable secondary structures that cannot be efficiently resolved by the reovirus RNA-dependent RNA polymerase. This may result in template jumping or template switching, which could yield deletion transcripts. In the newly formed cores, these deletion transcripts may serve as templates for negative strand formation, and thereby result in deletion segments.

CONCLUDING REMARKS

We demonstrated that during the routine production of virus batches, recombinant reoviruses show a lower infectivity compared to wild-type Type 3 Dearing (wt T3D) and *jln* reoviruses. We showed that the overall morphologies of recombinant reovirus and wild-type reovirus are similar, but that there may be empty spots on the recombinant virus capsid. We proposed that the $\sigma 1$ protein is not stably built into the capsid. This may interfere with virus infection, possibly at a post-entry level.

Next to the reduced infectivity, we noticed the occasional occurrence of deletion mutants, in which (parts of) the transgene and sometimes reovirus-derived sequences were deleted. An overview of the observed S1 deletions can be found in Table 2. The deletion mutant reoviruses overgrew the transgene-containing reovirus population within a few passages, demonstrating that they have a growth advantage over the intact recombinant reoviruses. The deletions occurred despite the transgene-containing segments having a size similar to the wild-type S1 segment. The deletions ranged from 47 to 519 nucleotides in size, showing that S1 segments with a smaller size than usual (as small as 897 base pairs) can be successfully packaged into virions. We speculated about the mechanisms underlying the deletions. We found no evidence for the involvement of splicing or homology-directed mechanisms. Furthermore, the deletions are unlikely caused by replacing the $\sigma 1$ head domain, removing the A- and B-boxes, or by adverse effects of the transgene-encoded protein. Although speculative, we propose that the most likely mechanism underlying the deletions is that complexities in the RNA structure may provoke template jumping of the RNA-dependent RNA polymerase and loss of S1 sequences. Interestingly, a similar mechanism was proposed before to underlie M1 deletions arising during the passaging of T1L/T3D reovirus reassortants [27]. Like for the deletion mutants we describe, these reassortants overgrew the virus populations upon propagation and the authors speculated too on the involvement

of secondary RNA structures. Moreover, difficulties in obtaining reoviruses expressing relatively long heterologous sequence stretches have also been attributed to complexities in the RNA structure [28]. These issues could be tackled by wobble-mutagenizing the constructs in order to reduce complexities in RNA secondary structure. Possibly, this could be attempted for our recombinant S1 constructs as well.

Virus clone	Deletion	Length	1st observ.	# observ.	Selective advantage
rS1-iLOV del1	GGCGCAACTG CGCCTCAGTA	464bp	Passage #10	1	Yes
rS1-iLOV del2	ATCACCGACC GGAGTACTTC	385bp	Passage #3	1	Yes
rS1-E4orf4 del1	GTCTCGGGCGC CGCCTCAGTA	47bp	Passage #3	Several	Yes
rS1-RFA	<i>No deletions found in any of the batches, up to 10 passages</i>				
rS1-hsGMCSF del1	AAAACCCCGG GCAGCACTGC	329bp	Passage #2	1	Yes
rS1-hsGMCSF del2	AAAGCAAGCA GGGCAGCCTC	298bp	Passage #2	2	Yes
rS1-hsGMCSF del3	ATAGGCGCAA CTTTGACTGC	519bp	Passage #2	1	Yes
rS1-hsGMCSFco del1	ATTCTATCAA TAATGTATT	230bp	Passage #2	1	Yes
rS1-hsGMCSFco del2	ATGTGGCTTC GCAGGGCCTT	249bp	Passage #2	2	Yes
rS1-hsGMCSFco del3	ATGTGGCTTC TGTGCTACTC	346bp	Passage #2	1	Yes
rS1-hsGMCSFco del4	ATGTGGCTTC CTA CTACAGAT	350bp	Passage #2	2	Yes
rS1-hsGMCSFco del5	GAAGAAAACC CAGGGCCTTA	268bp	Passage #2	1	Yes
rS1-hsGMCSFco del6	GAAGAAAACC GCTTCACATT	319bp	Passage #2	1	Yes
rS1-mmGMCSF	<i>No deletions found in any of the batches, up to 10 passages</i>				
rS1-dsRed	<i>No virus obtained despite several attempts</i>				
rS1-GaussiaLuc	<i>No virus obtained despite several attempts</i>				

Table 2. Overview of deletion mutant characteristics. Table showing the different recombinant reoviruses, the obtained deletion mutants, the deleted sequences, the length of the deletions, the passage number at which the deletion was first observed, the number of independent observations of this specific deletion, and whether the deletion mutant had a growth advantage over the reovirus harboring the intact S1 segment.

We did not examine whether the transgene-encoding S1 segments (and the other segments) are efficiently packaged into the recombinant reovirus particles. However, the $\sigma 1$ expression levels were similar in cell cultures infected with recombinant reoviruses compared to wt T3D or *jin* reoviruses (data not shown). This indicates that the S1 segments are expressed in infected cells, and therefore must have been present in the incoming reovirus particles. Therefore, we concluded that packaging of S1 is not hampered by encoding a transgene. Nevertheless, it remains to be determined whether the transgene-encoding S1 segments are efficiently packaged in every virus particle.

To our best knowledge, we are the first to discuss S1 deletions occurring in recombinant reoviruses through reverse genetics. Our findings highlight that routine monitoring of the integrity of the transgene-containing reoviruses is essential when generating batches of replication-competent reoviruses containing heterologous transgenes. We demonstrate that small- and medium-scale batches of recombinant reoviruses can be generated with relative ease. Moreover, the deletion mutants reveal the minimally required sequences for efficient packaging of modified segments into reovirus capsids.



REFERENCES

1. Schiff, L.A.; Nibert, M.L.; Tyler, K.L. Orthoreoviruses and their replication. *Fields Virology* **2007**, 5th edition, 1853–1915.
2. Gong, J.; Sachdev, E.; Mita, A.C.; Mita, M.M. Clinical development of reovirus for cancer therapy: An oncolytic virus with immune-mediated antitumor activity. *World J Methodol* **2016**, *6*, 25-42.
3. van den Wollenberg, D.J.; Dautzenberg, I.J.; van den Hengel, S.K.; Cramer, S.J.; de Groot, R.J.; Hoeben, R.C. Isolation of reovirus T3D mutants capable of infecting human tumor cells independent of junction adhesion molecule-A. *PLoS One* **2012**, *7*, e48064.
4. Leone, G.; Duncan, R.; Mah, D.C.W.; Price, A.; Cashdollar, L.W.; Lee, P.W.K. The N-terminal heptad repeat region of reovirus cell attachment protein $\sigma 1$ is responsible for $\sigma 1$ oligomer stability and possesses intrinsic oligomerization function. *Virology* **1991**, *182*, 336-345.
5. van den Wollenberg, D.J.; Dautzenberg, I.J.; Ros, W.; Lipinska, A.D.; van den Hengel, S.K.; Hoeben, R.C. Replicating reoviruses with a transgene replacing the codons for the head domain of the viral spike. *Gene Ther* **2015**, *22*, 267-79.
6. Kemp, V.; Dautzenberg, I.J.C.; Cramer, S.J.; Hoeben, R.C.; van den Wollenberg, D.J.M. Characterization of a replicating expanded tropism oncolytic reovirus carrying the adenovirus E4orf4 gene. *Gene Therapy* **2018**, *25*, 331–34.
7. Kemp, V.; van den Wollenberg, D.J.M.; Camps, M.G.M.; van Hall, T.; Kinderman, P.; Pronk-van Montfoort, N.; Hoeben, R.C., Arming oncolytic reovirus with GM-CSF gene to enhance immunity. *Cancer Gene Ther* **2019**, doi: 10.1038/s41417-018-0063-9.
8. Fallaux, F.J.; Kranenburg, O.; Cramer, S.J.; Houweling, A.; Van Ormondt, H.; Hoeben, R.C.; Van Der Eb, A.J. Characterization of 911: a new helper cell line for the titration and propagation of early region 1-deleted adenoviral vectors. *Hum Gene Ther* **1996**, *7*, 215-22.
9. Dautzenberg, I.J.; van den Wollenberg, D.J.; van den Hengel, S.K.; Limpens, R.W.; Barcena, M.; Koster, A.J.; Hoeben, R.C. Mammalian orthoreovirus T3D infects U-118 MG cell spheroids independent of junction adhesion molecule-A. *Gene Ther* **2014**, *21*, 609-17.
10. van den Wollenberg, D.J.; van den Hengel, S.K.; Dautzenberg, I.J.; Cramer, S.J.; Kranenburg, O.; Hoeben, R.C. A strategy for genetic modification of the spike-encoding segment of human reovirus T3D for reovirus targeting. *Gene Ther* **2008**, *15*, 1567-78.
11. Buchholz, U.J.; Finke, S.; Conzelmann, K.K. Generation of bovine respiratory syncytial virus (BRSV) from cDNA: BRSV NS2 is not essential for virus

- replication in tissue culture, and the human RSV leader region acts as a functional BRSV genome promoter. *J Virol* **1999**, *73*, 251-9.
12. Ni, Y.W.; Kemp, M.C. Subgenomic S1 Segments Are Packaged by Avian Reovirus Defective Interfering Particles Having an S1 Segment Deletion. *Virus Res* **1994**, *32*, 329-342.
 13. Roner, M.R.; Roehr, J. The 3' sequences required for incorporation of an engineered ssRNA into the Reovirus genome. *Virology* **2006**, *3*, 1.
 14. Roner, M.R.; Steele, B.G. Features of the mammalian orthoreovirus 3' Dearing I1 single-stranded RNA that direct packaging and serotype restriction. *J Gen Virol* **2007**, *88*, 3401-12.
 15. Boehme, K.W.; Ikizler, M.; Kobayashi, T.; Dermody, T.S. Reverse genetics for mammalian reovirus. *Methods* **2011**, *55*, 109-13.
 16. Kobayashi, T.; Antar, A.A.; Boehme, K.W.; Danthi, P.; Eby, E.A.; Guglielmi, K.M.; Holm, G.H.; Johnson, E.M.; Maginnis, M.S.; Naik, S. *et al.* A plasmid-based reverse genetics system for animal double-stranded RNA viruses. *Cell Host Microbe* **2007**, *1*, 147-57.
 17. Virgin, H.W.; Mann, M.A.; Fields, B.N.; Tyler, K.L. Monoclonal-Antibodies to Reovirus Reveal Structure-Function-Relationships between Capsid Proteins and Genetics of Susceptibility to Antibody Action. *Journal of Virology* **1991**, *65*, 6772-6781.
 18. Kupgan, G.; Hentges, D.C.; Muschinske, N.J.; Picking, W.D.; Picking, W.L.; Ramsey, J.D. The effect of fiber truncations on the stability of adenovirus type 5. *Mol Biotechnol* **2014**, *56*, 979-91.
 19. Maginnis, M.S.; Forrest, J.C.; Kopecky-Bromberg, S.A.; Dickeson, S.K.; Santoro, S.A.; Zutter, M.M.; Nemerow, G.R.; Bergelson, J.M.; Dermody, T.S. Beta1 integrin mediates internalization of mammalian reovirus. *J Virol* **2006**, *80*, 2760-70.
 20. Kim, M.; Garant, K.A.; zur Nieden, N.I.; Alain, T.; Loken, S.D.; Urbanski, S.J.; Forsyth, P.A.; Rancourt, D.E.; Lee, P.W.; Johnston, R.N. Attenuated reovirus displays oncolysis with reduced host toxicity. *Br J Cancer* **2011**, *104*, 290-9.
 21. Bokiej, M.; Ogden, K.M.; Ikizler, M.; Reiter, D.M.; Stehle, T.; Dermody, T.S. Optimum length and flexibility of reovirus attachment protein sigma1 are required for efficient viral infection. *J Virol* **2012**, *86*, 10270-80.
 22. Larson, S.M.; Antczak, J.B.; Joklik, W.K. Reovirus Exists in the Form of 13 Particle Species That Differ in Their Content of Protein Sigma-1. *Virology* **1994**, *201*, 303-311.
 23. Shayakhmetov, D.M.; Lieber, A. Dependence of adenovirus infectivity on length of the fiber shaft domain. *J Virol* **2000**, *74*, 10274-86.

24. Chappell, J.D.; Barton, E.S.; Smith, T.H.; Baer, G.S.; Duong, D.T.; Nibert, M.L.; Dermody, T.S. Cleavage susceptibility of reovirus attachment protein sigma 1 during proteolytic disassembly of virions is determined by a sequence polymorphism in the sigma 1 neck. *Journal of Virology* **1998**, *72*, 8205-8213.
25. Metcalf, D. The molecular biology and functions of the granulocyte-macrophage colony-stimulating factors. *Blood* **1986**, *67*, 257-67.
26. Buckley, P.T.; Khaladkar, M.; Kim, J.; Eberwine, J. Cytoplasmic intron retention, function, splicing, and the sentinel RNA hypothesis. *Wiley Interdiscip Rev RNA* **2014**, *5*, 223-30.
27. Zou, S.; Brown, E.G. Identification of sequence elements containing signals for replication and encapsidation of the reovirus M1 genome segment. *Virology* **1992**, *186*, 377-88.
28. Demidenko, A.A.; Blattman, J.N.; Blattman, N.N.; Greenberg, P.D.; Nibert, M.L. Engineering recombinant reoviruses with tandem repeats and a tetravirus 2A-like element for exogenous polypeptide expression. *Proc Natl Acad Sci U S A* **2013**, *110*, E1867-76.

